



Universiteit
Leiden
The Netherlands

Image processing and lattice determination for three-dimensional nanocrystals

Jiang, L.H.; Georgieva, D.; Nederlof, I.; Liu, Z.F.; Abrahams, J.P.

Citation

Jiang, L. H., Georgieva, D., Nederlof, I., Liu, Z. F., & Abrahams, J. P. (2011). Image processing and lattice determination for three-dimensional nanocrystals. *Microscopy And Microanalysis*, 17(6), 879-885. doi:10.1017/S1431927611012244

Version: Publisher's Version

License: [Licensed under Article 25fa Copyright Act/Law \(Amendment Taverne\)](#)

Downloaded from: <https://hdl.handle.net/1887/3620665>

Note: To cite this publication please use the final published version (if applicable).

Image Processing and Lattice Determination for Three-Dimensional Nanocrystals

Linhua Jiang, Dilyana Georgieva, Igor Nederlof, Zunfeng Liu, Jan Pieter Abrahams

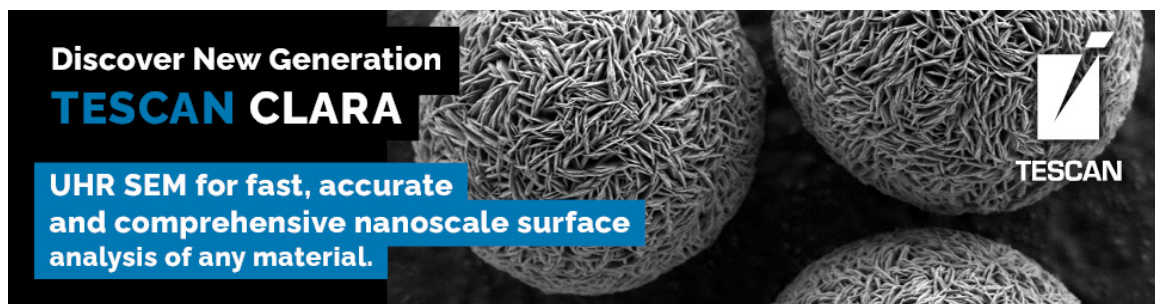


Image Processing and Lattice Determination for Three-Dimensional Nanocrystals

Linhua Jiang,^{1,2,*} Dilyana Georgieva,¹ Igor Nederlof,¹ Zunfeng Liu,¹ and Jan Pieter Abrahams^{1,*}

¹*Gorlaeus Laboratory, Faculty of Science, Leiden University, Einsteinweg 55, 2333 CC Leiden, The Netherlands*

²*Service Science Research Center, Shanghai Advanced Research Institute, Chinese Academy of Sciences, Shanghai 201203, China*

Abstract: Three-dimensional nanocrystals can be studied by electron diffraction using transmission cryo-electron microscopy. For molecular structure determination of proteins, such nanosized crystalline samples are out of reach for traditional single-crystal X-ray crystallography. For the study of materials that are not sensitive to the electron beam, software has been developed for determining the crystal lattice and orientation parameters. These methods require radiation-hard materials that survive careful orienting of the crystals and measuring diffraction of one and the same crystal from different, but known directions. However, as such methods can only deal with well-oriented crystalline samples, a problem exists for three-dimensional (3D) crystals of proteins and other radiation sensitive materials that do not survive careful rotational alignment in the electron microscope. Here, we discuss our newly released software AMP that can deal with nonoriented diffraction patterns, and we discuss the progress of our new preprocessing program that uses autocorrelation patterns of diffraction images for lattice determination and indexing of 3D nanocrystals.

Key words: electron diffraction, 3D nanocrystals, image processing, lattice determination, protein crystals, cryo-EM

INTRODUCTION

When the electron beam in a transmission electron microscope (TEM) passes through a thin (e.g., <100 nm) crystalline layer, the electrons scatter and interfere with each other and (if the microscope is set to the proper mode) a diffraction pattern can be observed on a fluorescent screen or be recorded on film, image plate (Fig. 1), or a charge-coupled device camera. The constructive interference of the electrons focused as spots in a diffraction pattern is described by Bragg's law (Bragg, 1913), which is the basis of electron diffraction and structural reconstruction in electron crystallography.

Electron diffraction is widely used in material science, and it is gaining significance in life science for studying two-dimensional (2D) and three-dimensional (3D) protein crystals. It has been successfully used for structure determination of crystalline materials in inorganic material research and also for solving molecular structures of 2D crystals of transmembrane proteins (Fujiyoshi & Unwin, 2008). Atomic models for several membrane proteins have been successfully determined, for instance, bacteriorhodopsin (BR) (Henderson et al., 1990), aquaporin 4 (AQP4) (Hiroaki et al., 2006), and microsomal glutathione transferase 1 (MGST1) (Holm et al., 2006); also the structure of the water soluble tubulin could be solved using 2D electron crystallography (Nogales et al., 1998). In material science, electron crystallography is used to solve structures of inorganic materials (McQueen et al., 2007; Mugnaioli et al., 2009; Sun et al., 2010). However, radiation sensitive 3D

organic nanocrystals, especially 3D protein nanocrystals, have largely been considered as unsuitable.

It would be very attractive if electron diffraction could be used for studying 3D organic (protein) nanocrystals (see Fig. 1a,b). Such crystals are often more easy to grow than multimicrometer-sized crystals, which are a prerequisite for X-ray crystallographic studies. In many cases, nanocrystals may be the only samples that we can get. Given its potential, 3D electron nanocrystallography as a new method of biomolecular structure determination is receiving increasing interest (Zou et al., 2004; Jiang et al., 2009b).

There are still some serious technical obstacles that need to be overcome before electron diffraction of 3D protein crystals can be used for structure determination. Challenges include dynamic scattering and low signal-to-noise ratios, as prolonged exposure by the electron beam may destroy the crystals. With current electron detector technologies, the beam sensitivity of protein crystals prevents collecting multiple exposures, as in standard X-ray crystallography or in electron tomography. However, a new noise-free quantum area detector—Medipix^a—is being developed that may ease this problem (Plaisier et al., 2003). If successful, ultralow dose exposure may allow the collection of multiple diffraction frames, but it will produce diffraction patterns with very low signal-to-noise ratios.

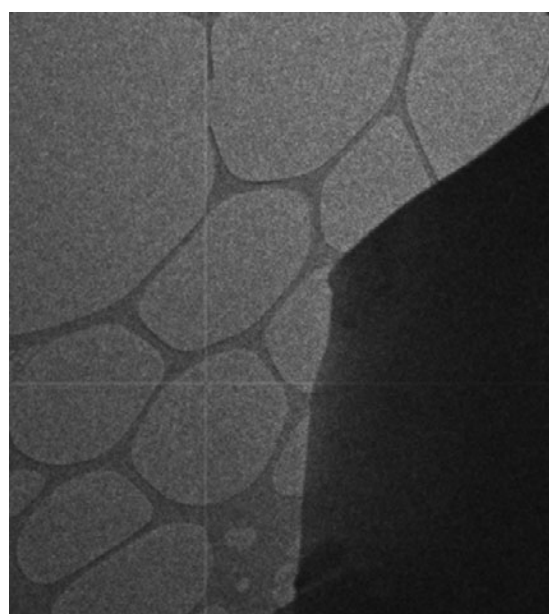
Electron diffraction data analysis is different from that in X-ray crystallography, although many principles are the same. Both require the following steps:

1. Background removal and spot localization. The diffraction patterns need to be centered and in electron diffrac-

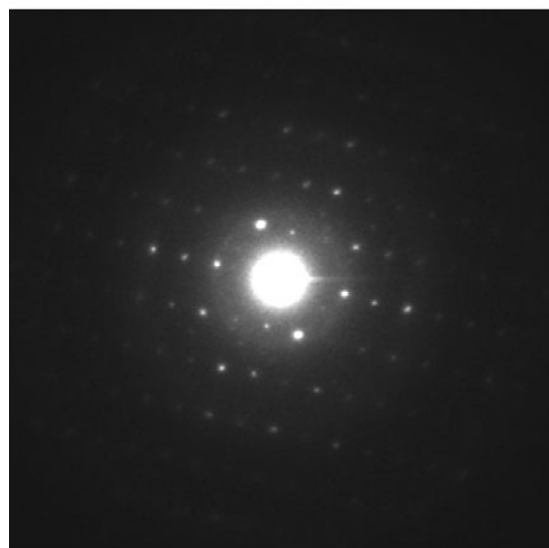
Received July 13, 2011; accepted August 16, 2011

*Corresponding authors. E-mail: ljiang@science.leidenuniv.nl; Abrahams@science.leidenuniv.nl

^aAvailable at www.medipix.web.cern.ch/MEDIPIX/.



(a)



(b)

Figure 1. **a:** A 3D nanocrystal of tryptophan lying on the carbon support. **b:** An electron diffraction pattern of a 3D nanocrystal of lysozyme. The diffraction pattern shows a regular, symmetric lattice because of the low curvature of the Ewald sphere relative to the maximum resolution of diffraction.

tion, the strong background caused by the undiffracted electron beam needs to be dealt with. If a beam-stop exists, its shadow should be taken into account. Then one needs to locate the diffraction spots, extract the coordinates of their centroids, and calculate the intensities of the spots in the pattern for lattice determination by characterizing the principal vectors V_1 and V_2 corresponding to the basic spacing of the spot coordinates.

2. Unit-cell determination. Unit-cell determination of radiation-hard, well-oriented crystals by electron diffraction is not very difficult (Li, 2005; Kolb et al., 2008) and also unit-cell determination using multiple diffraction pat-

terns in random orientations is straightforward, provided the rotation angles of the frames are accurately known. However, determining the unit-cell parameters from randomly oriented diffraction patterns from different crystals, without knowledge of their angular relationships, required creating a new algorithm (Jiang et al., 2009b).

3. Indexing and intensity integration. Once the unit cell is known, the rotation angles of the randomly oriented diffraction patterns need to be determined, using the unit cell found in the previous step. This indexes the reflections of every electron diffraction image. The intensity of each spot is then calculated with greater accuracy than in step 1 using an intensity integration procedure.
4. Phase recovery and structure refinement. When the indices and their corresponding intensity are known, methods from X-ray crystallography can be used to reconstruct the 3D lattice of intensities in reciprocal space. Phase recovery of electron diffraction (Abrahams, 2010) may be facilitated by dynamical scattering effects but requires knowledge of the orientation parameters for each recorded intensity, which means that standard X-ray crystallography data integration software may not be used for this purpose. Subsequent iterative refinement is essential for determining the atomic structure and may involve correction for dynamical scattering.

For the first steps in crystal data processing, well-established software is available for X-ray crystallography, for instance the CCP4 suite (Collaborative, 1994; Winn, 2003). A few programs (Table 1) are specially designed for electron crystallography (MRC programs: Crowther et al., 1996; 2dx: Gipson et al., 2007 and Calidris^b; TRICE: Zou et al., 2004; DiffTools: Mitchell, 2008, DIFPACK,^c and IPLT^d).

However, none of these programs handle the electron diffraction data of 3D radiation sensitive crystals.

METHODS AND RESULTS

Locating Spots

When neither the lattice parameters nor the orientation of the crystal(s) are known, image processing routines are used for finding the location of the diffraction spots. Typical image processing software for electron diffraction data centers diffraction patterns, removes the background, and automatically locates peaks (Mitchell, 2008). Advanced functions include determining the spacing between spots and angle determination between vectors defined by pairs of spots, fitting the spots to a regular lattice pattern, and calculating rotational averaged profiles. General image processing techniques, such as image enhancement and Gaussian filters, are usually employed for these tasks.

Our recent progress includes the development of advanced procedures for peak searching, 2D lattice determina-

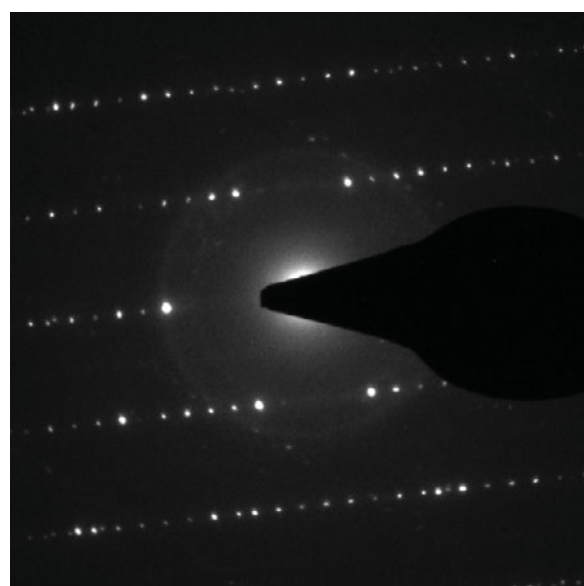
^b Available at www.calidris-em.com/.

^c Available at www.gatan.com/imaging/difpac.php.

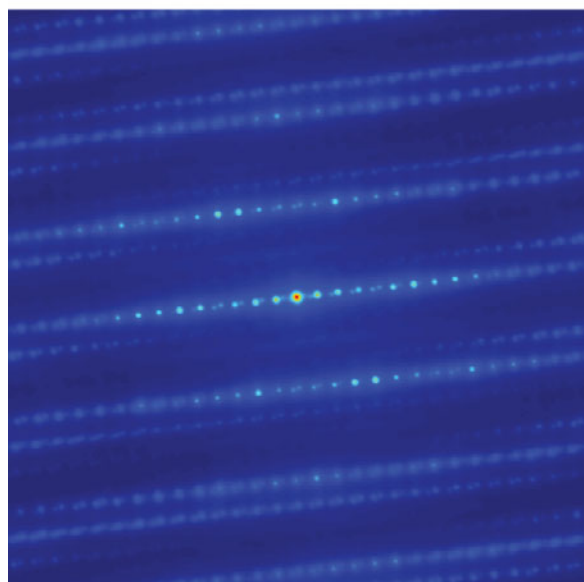
^d Available at www.iplt.org/.

Table 1. Scientific Programs Available for Electron Crystallography.

Software Name	Description	Copyright
MRC programs	General software package for electron and X-ray crystallography	Free
2dx	Software for processing of 2D crystal images	Free
Calidris (CRISP, ELD, TRICE, etc.)	Software for image processing of 3D crystal data	Commercial
DiffTools	Software platform used in TEM	Free
DIFPACK™	Tools to calibrate diffractograms, measure d-spacings and angles, etc.	Commercial
IPLT	Image Processing Library & Toolbox emphasis on 2D electron crystallography	Free



(a)



(b)

Figure 2. **a:** An example of electron diffraction image of aspirin with a beam-stop shadow, recorded on an image plate. **b:** The autocorrelation map of background and beam-stop removed image of panel **a**.

tion, and determining the 3D unit-cell parameters (Jiang et al., 2009b) that also work in the absence of knowledge of lattice constants or crystal settings. We developed a user-friendly peak search program, called AMP (Autocorrelation Mapping Program),^e in which an autocorrelation algorithm is utilized for intensifying the signal and centering the image on the apparent lattice [(Jiang et al., 2009a), Fig. 2]. AMP processes diffraction images of 3D nanocrystals and automatically finds peak positions. First, the program centers the image and removes its background that includes the strong central beam and possible backstop shadow. Then it creates an autocorrelation map filling up weak or missing reflections, enhancing the signal-to-noise ratio and centering the diffraction pattern (Fig. 2b). The autocorrelation method relies on the 2D lattice features apparent in the electron diffraction patterns. The slight curvature of the Ewald sphere in these electron diffraction patterns does not create difficulties in this particular application because the autocorrelation map is only used as a reference and acts as a template for searching peaks in the original images. We have found this method to be extremely robust, even when dealing with apparently irregular patterns and twinned, mixed lattices.

The distinguishing idea of our peak searching program AMP is the use of autocorrelation maps for intensifying the signal and centering the original diffraction pattern. Intensifying the signal is important for improving the signal-to-noise ratio as well as for identifying diffraction spots, which are masked by the backstop or buried under noise. The algorithm shows improved performance especially when the noise is high. Another advantage is that the autocorrelation pattern is accurately centered by definition. It solves the problem of finding the exact center of the original diffraction image under the cover of a strong direct beam (Fig. 1b) or backstop (Fig. 2a).

Both the original electron diffraction pattern and its autocorrelation pattern need to be corrected for diffuse background signals. The level and nature of the background noise are very different for different types of images; hence, a more clever background removal algorithm is required, rather than straightforward fixed-threshold methods. We

^e Available at www.bfsc.leidenuniv.nl/software/.



Figure 3. The result of image background removal, centering, and spot localization of the image in Figure 2a. Recognized diffraction spots are marked by circles.

found it better to employ statistical features (e.g., rotationally averaged images and variance curves) for removing background noise, resulting in an adaptive background removal method (Jiang et al., 2009a). Although the signal of the autocorrelation images is stronger, the noise from the original image is still present, affecting the peak search accuracy. The adaptive background removal method needs to be applied on both the original diffraction image and its autocorrelation image. The only difference is that the radial central beam (or the shadow of beam-stop) does not need to be removed from the autocorrelation image. A multistep procedure, which includes the radial central beam removal, low- and high-pass Gaussian filtering, is employed in this method to erase the background. One of the centering and peak searching results is shown in Figure 3.

The program AMP was designed to be user-friendly. It allows visualizing all the images that are being processed in the peak search procedure. A graphical user interface is implemented, providing the users a simple way to run, control, and monitor the image processing. The program was written in Matlab and has been compiled into a stand-alone executable program.

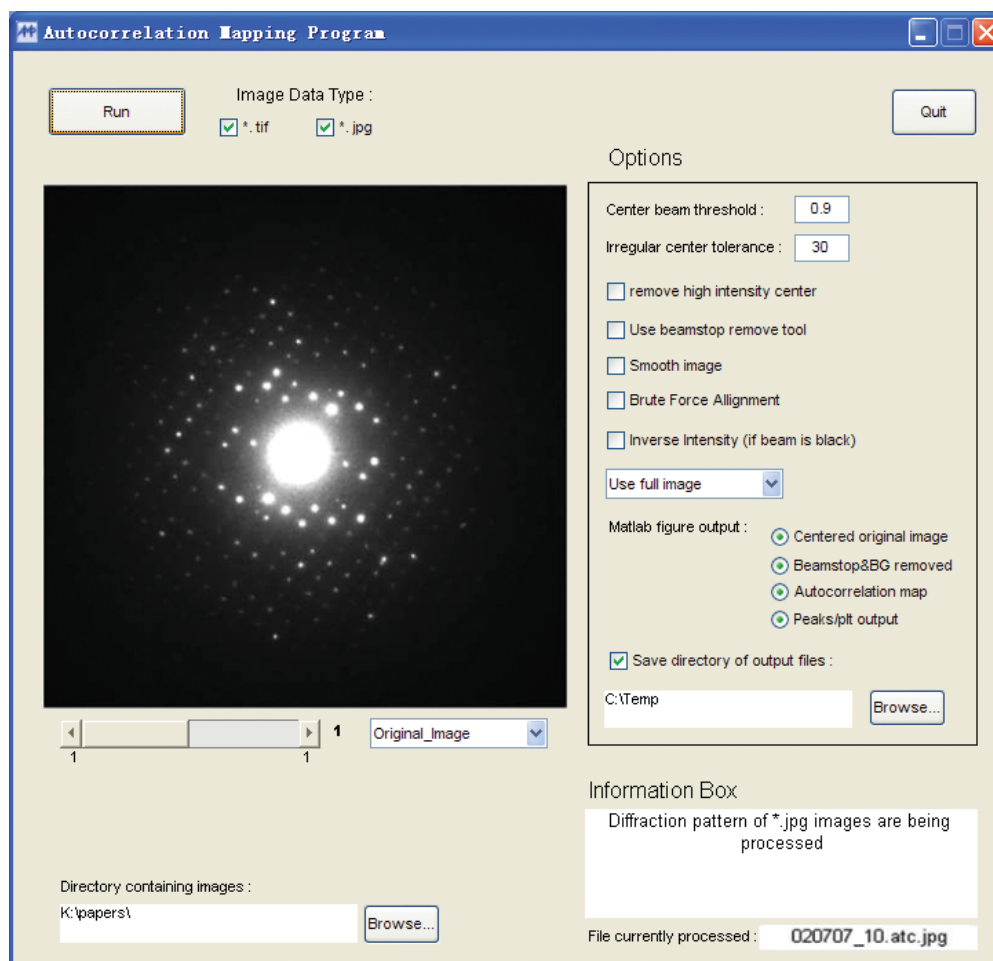


Figure 4. Graphical user interface of the newest version of AMP (version v1.8) for electron diffraction image processing. The image displayed on the left is a digital electron diffraction image of an oxacillin nanocrystal. The panel right of the image allows setting input and output of parameters.

Figure 4 shows a screenshot of the most recent version of AMP. The diffraction image that is being processed is visible on the left, and more options and controls are provided to the user on the right of the panel. Except for the necessary input parameters, the user can select which intermediate output needs to be checked visually during processing. Notices and information concerning the run of diffraction patterns that is processed is shown on the bottom right. Currently, AMP supports TIFF (up to 16-bit and 32-bit deep) and JPEG image formats, which are the most widely-used formats for storing digital images. Other image formats can be easily supported.

The autocorrelation map and peak coordinates generated by the program can be used as input files for subsequent unit cell determination of the nanocrystals (Jiang et al., 2009b).

2D Lattice and Main Vectors Determination via Linear Multiregression

Compared to X-ray diffraction, electron diffraction patterns have different features due to the rather short wavelength of the electron beam compared to the dimensions of unit cell and typical resolution of protein crystals. More regular lattices without clear Laue rings are hence observed. Because in electron diffraction studies by TEM the Ewald sphere is very flat, at lower resolution (2–3 Å), we mainly observe 2D lattices with crystallographic zones located in stripes, separated by bands devoid of diffraction spots. Hence, there are parallels with lattice determination in 2D protein crystallography (Zeng et al., 2007). For calculating the autocorrelation pattern discussed above, an inverse fast Fourier transform is multiplied with its complex conjugate. The autocorrelation pattern results upon a forward Fourier transform. Since the spots are regularly distributed in the electron diffraction pattern, the spacing between the spots is also regular. The autocorrelation pattern of this image will therefore also show a regular lattice with the same spacing.

In crystallographic data, diffraction spots may be very weak or even missing due to the crystal (pseudo-)symmetry, unit-cell contents, beam damage, crystal imperfections, the strong central beam, or high noise (also see Figs. 1b, 2a). However, once we know the lattice, we know where to locate the peaks more accurately, allowing, for instance, profile fitting for accurate intensity determination. Hence, finding this lattice is paramount. As explained in the previous paragraph, the lattice of the autocorrelation pattern is identical to the lattice of the diffraction pattern, but the spots of the autocorrelation patterns are much better resolved than that of the diffraction pattern. Hence, we use the autocorrelation patterns for the lattice determination.

The spots have two types of information: the coordinates and the intensity. For the coordinates of spots on a lattice, the most principal information is encoded by the base vectors V_1 and V_2 and the index of the spot (given by a pair of whole integers). The base vectors in electron diffraction are very useful in determination of the unit-cell

parameters, and their identification forms the first step in determination of the structure of a crystal.

The strategy for determining unit cells involves simulating all possible lattices by combining any pair of reasonable base vectors V_1 and V_2 , and then calculating the fitting score of this simulated lattice with the observed lattice, identifying the base vectors with the maximum score in an exhaustive search. The pair of vectors V_1' and V_2' that result from this exhaustive search is only approximate, as the brute force search is discrete by necessity. To have a more accurate determination of the base vectors, linear multiregression of all spots along a single line is employed to refine each vector's length. An additional linear multiregression of all of the spots in the pattern can be applied to further push the accuracy.

Mathematically,

$$\vec{D}_i = M_i \vec{V}_1 + N_i \vec{V}_2 + \vec{C} + \vec{\epsilon}_i. \quad (1)$$

Here, \vec{D}_i is the i 'th vector corresponding to the i 'th diffraction spot, and M_i and N_i are its 2D integer indexing numbers, to be multiplied by the approximated base vectors V_1' and V_2' (note that M_i and N_i are not necessarily related to the 3D reciprocal HKL indexing numbers, as the diffraction pattern may be of a random zone). \vec{C} is the center of the diffraction or autocorrelation pattern and $\vec{\epsilon}_i$ is random noise.

Transforming the vectors to the X and Y coordinates in the plane,

$$X_{Di} = M_i X_{V1} + N_i X_{V2} + X_C + X_{\epsilon i}, \quad (2)$$

$$Y_{Di} = M_i Y_{V1} + N_i Y_{V2} + Y_C + Y_{\epsilon i}. \quad (3)$$

We can rewrite equation (2) in matrix form, allowing linear regression:

$$\begin{pmatrix} M_1 & N_1 & 1 \\ M_2 & N_2 & 1 \\ \dots & \dots & \dots \\ M_n & N_n & 1 \end{pmatrix} \begin{pmatrix} X_{V1} \\ X_{V2} \\ X_C \end{pmatrix} = \begin{pmatrix} X_{D1} \\ X_{D2} \\ \dots \\ X_{Dn} \end{pmatrix}. \quad (4)$$

Equation (4) allows standard linear multiregression for calculating the coordinates of the base vectors and beam center: X_{V1} , X_{V2} and X_C .

The same method applied in equation (3) obviously also works for determining the optimal Y coordinates.

Accuracy can be improved by excluding false positive spots that deviate too much from the lattice, as they affect the regression analysis. Our program allows more interactive refinement by manual exclusion of wrongly identified diffraction spots in the spot searching step. In this way, very accurate results can be achieved (Fig. 5 and Table 2). Measures of error—e.g., an R -factor—can be calculated to evaluate the fitting. After the refinement, we have found fitting of the resulting lattice to be accurate enough for the next step of unit-cell determination. This part of algorithm was implemented in our program EDiff (to be released). A gross error tolerance can be set by the user in the program, normally 0.5–2%. For accurate correction of the magnifica-

Table 2. Part of the Experimental Results of Lattice and Main Vectors Determination of Lysozyme Electron Diffraction Data.*

Image Serial Number	Number of Peaks/ False Positive	Main Vectors (\AA^{-1})	Angle between Main Vectors ($^{\circ}$)	Lattice Fitting Errors (%)
1	116/1	43.66, 29.18	88.53	0.77
2	142/1	44.99, 29.30	89.96	0.79
3	87/1	44.03, 29.92	88.95	0.49
4	107/2	43.42, 30.60	89.31	1.02
5	100/2	42.79, 29.80	87.24	1.01

*The results show that our program extracted the diffraction peaks successfully, and the lattice was determined with tolerable low errors.

tion error present in electron microscopes, a suggested method is looking down the fourfold axis of a cubic or tetragonal crystal (Capitani et al., 2006).

DISCUSSION AND CONCLUSION

The idea of using autocorrelation patterns for intensifying the signal, accurately centering the pattern, and for filling up the missing spots was shown here to be useful. This new idea makes use of the regular lattices observed in electron diffraction patterns that are due to a combination of a short electron wavelength and a relatively low maximum resolution of diffraction (typical for 3D protein crystals). Moreover, a method of adaptive background removal was designed and implemented in the automatic peak searching program for accurate spot localization.

The peak searching program is available as a free pre-processing program for analyzing electron diffraction data of nanocrystals (AMP; see footnote e on p. 881). It yields

stable results during the test of various types of experimental images. The results of the program provide a solid base for further data analysis and structure determination of 3D protein nanocrystals, including unit-cell determination of crystalline materials.

Refining the lattice base vectors of using linear regression was shown to be robust and is an essential step for unit-cell determination and subsequent indexing in 3D reciprocal space later. A user-friendly indexing and intensity integration program is currently under development and will be reported on shortly.

For testing our program, different types of experimental image data were used, including data from both organic and inorganic nanocrystals: lysozyme, tryptophan, aspirin, penicillin, mayenite, etc. More than 500 diffractograms in total were tested. Part of these patterns can be downloaded from our website for testing. The results showed a high level of performance of our new program: it was able to correctly identify the diffraction reflections even in the presence of high background noise or (relatively) huge backstop shadows present in the original diffraction patterns. Subsequent 2D lattice determination for retrieving the base vectors V_1 and V_2 for unit-cell determination was successful. We conclude that we have made another step forward in accurate processing of random 3D electron diffraction data.

ACKNOWLEDGMENTS

This research was financially supported by a NOW (The Netherlands Organisation for Scientific Research) top grant. Part of the research was also supported by the funding of Cyttron I and II (www.cyttron.org/).

REFERENCES

- ABRAHAMS, J.P. (2010). The strong phase object approximation may allow extending crystallographic phases of dynamical electron diffraction patterns of 3D protein nano-crystals. *Z Kristallogr* **255**, 67–76.
- BRAGG, W.L. (1913). The diffraction of short electromagnetic waves by a crystal. *Proc Camb Phil Soc* **17**, 43–57.
- CAPITANI, G. C., OLEYNIKOV, P., HOVMÖLLER, S. & MELLINI, M. (2006). A practical method to detect and correct for lens distortion in the TEM. *Ultramicroscopy* **106**, 66–74.

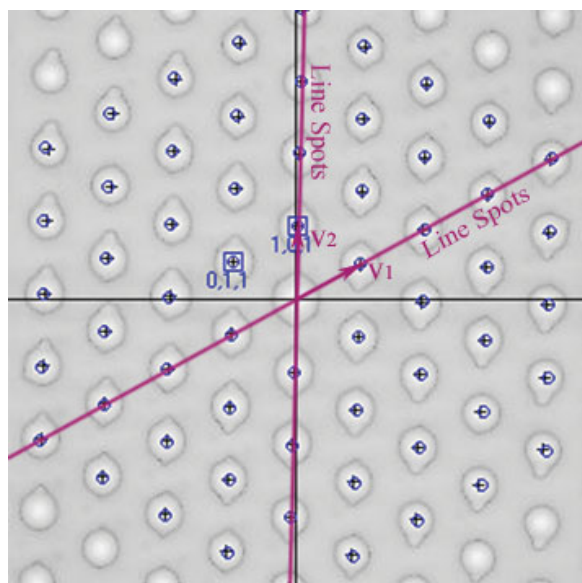


Figure 5. Linear multiregression of line spots and all spots to determination the vectors of a lattice. The base vectors V_1 and V_2 are determined and marked.

- COLLABORATIVE (1994). The CCP4 suite: Programs for protein crystallography. *Acta Crystallogr D* **50**, 760–763.
- CROWTHER, R.A., HENDERSON, R. & SMITH, J.M. (1996). MRC image processing programs. *J Struct Biol* **116**, 9–16.
- FUJIYOSHI, Y. & UNWIN, N. (2008). Electron crystallography of proteins in membranes. *Curr Opin Struct Biol* **18**, 587–592.
- GIPSON, B., ZENG, X., ZHANG, Z.Y. & STAHLBERG, H. (2007). 2dx—User-friendly image processing for 2D crystals. *J Struct Biol* **157**, 64–72.
- HENDERSON, R., BALDWIN, J.M., CESKA, T.A., ZEMLIN, F., BECKMANN, E. & DOWNING, K.H. (1990). Model for the structure of bacteriorhodopsin based on high-resolution electron cryomicroscopy. *J Molec Biol* **213**, 899–929.
- HIROAKI, Y., TANI, K., KAMEGAWA, A., GYOBU, N., NISHIKAWA, K., SUZUKI, H., WALZ, T., SASAKI, S., MITSUOKA, K., KIMURA, K., MIZOGUCHI, A. & FUJIYOSHI, Y. (2006). Implications of the aquaporin-4 structure on array formation and cell adhesion. *J Molec Biol* **355**, 628–639.
- HOLM, P.J., BHAKAT, P., JEGERSCHOLD, C., GYOBU, N., MITSUOKA, K., FUJIYOSHI, Y., MORGENSTERN, R. & HEBERT, H. (2006). Structural basis for detoxification and oxidative stress protection in membranes. *J Molec Biol* **360**, 934–945.
- JIANG, L., GEORGIEVA, D., IJSPEERT, K. & ABRAHAMS, J.P. (2009a). An intelligent peak search program for digital electron diffraction images of 3D nano-crystals. *CISP '09, 2nd International Congress*, October 17–19, 2009, pp. 1–5.
- JIANG, L.H., GEORGIEVA, D., ZANDBERGEN, H.W. & ABRAHAMS, J.P. (2009b). Unit-cell determination from randomly oriented electron-diffraction patterns. *Acta Crystallogr D* **65**, 625–632.
- KOLB, U., GORELIK, T. & OTTEN, M.T. (2008). Towards automated diffraction tomography. Part II—Cell parameter determination. *Ultramicroscopy* **108**, 763–772.
- LI, X.Z. (2005). Computer programs for unit-cell determination in electron diffraction experiments. *Ultramicroscopy* **102**, 269–277.
- MCQUEEN, T., XU, Q., ANDERSEN, E.N., ZANDBERGEN, H.W. & CAVA, R.J. (2007). Structures of the reduced niobium oxides Nb₁₂O₂₉ and Nb₂₂O₅₄. *J Solid State Chem* **180**, 2864–2870.
- MITCHELL, D.R.G. (2008). DiffTools: Electron diffraction software tools for DigitalMicrograph™. *Microsc Res Techniq* **71**, 588–593.
- MUGNAIOLI, E., GORELIK, T. & KOLB, U. (2009). “Ab initio” structure solution from electron diffraction data obtained by a combination of automated diffraction tomography and precession technique. *Ultramicroscopy* **109**, 758–765.
- NOGALES, E., WOLF, S.G. & DOWNING, K.H. (1998). Structure of the alpha beta tubulin dimer by electron crystallography. *Nature* **391**, 199–203.
- PLAISIER, J.R., KONING, R.I., KOERTEN, H.K., VAN ROON, A.M., THOMASSEN, E.A.J., KUIL, M.E., HENDRIX, J., BROENNIMANN, C., PANNU, N.S. & ABRAHAMS, J.P. (2003). Area detectors in structural biology. *Nucl Instrum Methods A* **509**, 274–282.
- SUN, J.L., HE, Z.B., HOVMÖLLER, S., ZOU, X.D., GRAMM, F., BAERLOCHER, C. & MCCUSKER, L.B. (2010). Structure determination of zeolite IM-5 by electron crystallography. *Z Kristallogr* **225**, 77–85.
- WINN, M. (2003). An overview of the CCP4 project in protein crystallography: An example of a collaborative project. *J Synchrotron Radiat* **10**, 23–25.
- ZENG, X., GIPSON, B., ZHENG, Z.Y., RENAULT, L. & STAHLBERG, H. (2007). Automatic lattice determination for two-dimensional crystal images. *J Struct Biol* **160**, 353–361.
- ZOU, X.D., HOVMOLLER, A. & HOVMOLLER, S. (2004). TRICE—A program for reconstructing 3D reciprocal space and determining unit-cell parameters. *Ultramicroscopy* **98**, 187–193.



TESCAN TENSOR

Integrated, Precession-Assisted,
Analytical 4D-STEM



Visit us and learn more
about our TESCAN TENSOR

info.tescan.com/stem